Hindawi
Advances in Civil Engineering
Volume 2019, Article ID 7682575, 10 pages
https://doi.org/10.1155/2019/7682575

Research Article

A Stress-Strain Model for Brick Prism under Uniaxial Compression

Keun-Hyeok Yang, Yongjei Lee, and Yong-Ha Hwang

Department of Architectural Engineering, Kyonggi University, Suwon 16227, Republic of Korea

Correspondence should be addressed to Yongjei Lee; yongjei@gmail.com

Received 25 November 2018; Revised 1 February 2019; Accepted 11 March 2019; Published 14 April 2019

Academic Editor: Carlos Chastre

This study proposes a simple and rational stress-strain relationship model applicable to brick masonry under compression. The brick prism compression tests were conducted with different mortar strengths and with constant brick strength. From the observation of the test results, shape of the stress-strain curve is assumed to be parabola. In developing the stress-strain model, the modulus of elasticity, the strain at peak stress, and the strain at 50% of the peak stress on the descending branch were formulated from regression analysis using test data. Numerical and statistical analyses were then performed to derive equations for the key parameter to determine the slopes at the ascending and descending branches of the stress-strain curve shape. The reliability of the proposed model was examined by comparisons with actual stress-strain curves obtained from the tests and the existing model. The proposed model in this study turned out to be more accurate and easier to handle than previous models so that it is expected to contribute towards the mathematical simplicity of analytical modeling.

1. Introduction

Masonry is a material built from units and mortar that induce an anisotropic behavior for the composite. The lack of knowledge on the properties of the composite material imposes low assessments of the strength capacity of the masonry wall. Atkinson et al. [1] state that the prediction of compressive and deformation of full-scale masonry based on compressive test of stack-bond masonry prism and the interpretation of the results prism tests have a significant influence on the allowable stress and stiffness used in the masonry design. When structural masonry is subjected to vertical and horizontal loading, one of the most important parameters for design is the stress-strain relationship. Especially, the stress-strain relationship of concrete brick prism in compression is essential for the analysis of masonry structures. The relationship is generally known to depend on several interrelated test parameters including compressive strength of bricks and mortar. Many mathematical models have been proposed for accurate finite element models and structural analysis of concretes in compression. Existing stress-strain models for concretes [2–5] used the basic expression established by Popovics [6] or Sargin et al. [7], and the constants in the basic expression were determined empirically. In some models, the ascending and descending branches were dealt with separately with nonlinear equations; in this case, the test data were essential to establish the empirical constants. Hence, some limitations such as applicable ranges of concrete strength and concrete density exist. Knutson [8] evaluated the stress-strain diagrams for various materials and showed that they can be cast into a mathematical form. However, Mohamad et al. [9] mentioned a complete understanding of the mechanisms involved in the deformation and failure which are not fully explained. It is believed that the development of a theoretical model of universal application is a rather hard task, although there have been very nice efforts to propose simplified mathematical models for the stress-stain relation [10, 11]. When modeling masonry structure in common FEM software such as Abaqus [12] and LS-DYNA [13], it is not possible to correctly model and predict the behavior of masonry structures primarily due to the lack of the

references that fully define the plastic behavior of masonry. In design process, just as in analysis, the accurate design code considering elastic and plastic properties of the masonry is not given, either.

Although the brittle materials such as concrete have similar issues, a model proposed by Yang et al. [14] explained the stress-strain behavior of it in compression quite successfully. The study calibrated the mathematical equation for the stress-strain curve using material test results. As mentioned above, the pure theoretical development for the behavior of the concrete brick prism is rather a difficult task. However, the theoretical approach with aid of the material test can make a satisfactory result. The present study aims to propose a simple and rational model for nonlinear stress-strain curves of concrete brick masonry in compression with various mortar strengths (f_m). For this model, a key parameter that determines the slopes of the ascending and descending branches is formulated using a parametric numerical analysis, where different mortar strengths are considered, including the modulus of elasticity and secant modulus joining the origin and the $0.5f_{pm}$ point after the peak stress, where f_{pm} is a strength of prism. For the material properties used to define the stress-strain relationship, a regression analysis is performed on an extensive amount of test data collected from a wide variety of concrete specimens. The reliability of the developed model is examined using a normalized root-mean-square error obtained from a comparison of model estimates with the experimental data. Finally, the existing empirical models are reviewed and compared with the developed model.

2. Experiment

2.1. Specimens. To evaluate the compressive strength of the concrete brick prism, the specimens (Figure 1) were prepared with three different mortar strengths: (1) twice of the minimum concrete brick strength (8 MPa) required by KS F404 [15]; named specimen Cp-2.0, (2) two and half times of the minimum concrete brick strength, named specimen Cp-2.5, and (3) three times of the minimum concrete brick strength, named specimen Cp-3.0. Here, the specimen notations include two parts as follows: the first part, "Cp," refers that the specimen is in compression and the second part refers to the mortar identification.

2.2. Materials. Before evaluating the strength of concrete brick prism, material test of each component, brick and mortar, was performed. The test protocol of compressive strength of standard concrete brick ($190 \times 90 \times 57$ mm) followed KS F404 [15]. The test result shows that the average compressive strength of 11 specimens was 8.23 MPa and the standard deviation of them was 0.198 (Table 1). The volumetric mixture ratio of cement and sand of the joint mortar was 1 : 2.7. The water-cement ratio was decided through the premixing procedure (Table 2). The cylindrical specimen ($\phi 100 \times 200$ mm) test result showed that the strength of the mortar was more than 10.8 MPa which is the minimum required mortar strength for masonry by KS L5220 [16]. The resulting compressive stress of the mortar was 2-3% more than the planned strength and also that of the concrete brick was 3% more than originally planned strength. As a result, the exact ratios of the mortar to concrete brick strength of Cp-2.0, Cp-2.5, and Cp-3.0 were 2.0, 2.4, and 2.8, respectively. As the compressive strength of mortar increased, the strain at the maximum strength decreased by 8.16% in $2.5f_b$ and 10.20% in $3.0f_b$, when they were compared to $2.0f_b$ (Table 3), where f_b is the strength of brick. The stress-strain relationship of mortars and brick is shown in Figure 2. The brick was the most ductile material among them showing the lowest strength but the highest strain.

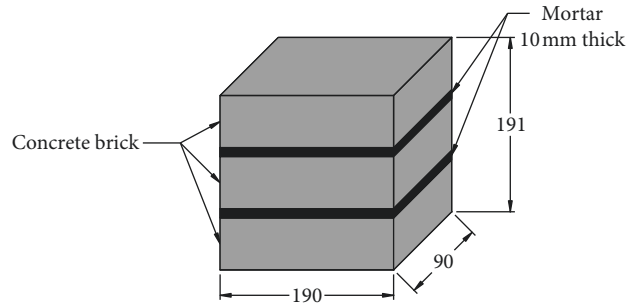

Figure 1: Masonry element for shear friction test (unit: mm).

Table 1: Compressive strength of bricks (MPa).

Identification of brick	f_{brick} (MPa)	Average of f_{brick} (MPa)	Standard deviation	Average strain at f_{brick}
1	8.265			
2	8.014			
3	8.522			
4	7.935			
5	8.071			
6	8.418	8.23	0.198	0.00248
7	8.091			
8	8.459			
9	8.092			
10	8.367			
11	8.249			

Note. f_{brick} = compressive strength of brick.

2.3. Loading and Measurement. The test specimens were prepared with caution to align the loading point with the center of the specimen to avoid eccentricity. Two linear variable differential transformers (LVDT) which can measure displacement up to 25 mm were installed at both sides of the prism (Figure 3). The data from each LVDT were compared to exam if there occurred any eccentricity. The load was applied by 500 kN capacity universal testing machine (UTM). The loading rate was 0.1 mm per minute.

3. Test Results and Discussion

3.1. Failure Mode. Typical failure mode by compression is shown in Figure 4. The first crack started at the brick near the steel attachment at 40%~50% of the peak stress. The number of cracks increased mainly around it. The cracks developed

Table 2: Compressive strength of mortars (MPa).

	Identification of mortar	W/C (%)	f_m (MPa)	Average of f_m (MPa)	Standard deviation	Strain at f_m, ε_0	Rate of strain change at f_m (%)
1			17.1				
2	$2.0f_b$	74.1	16.4	16.4	0.7	0.00245	—
3			15.7				
4			19.2				
5	$2.5f_b$	64.8	19.6	19.4	0.2	0.00225	−8.16
6			19.3				
7			23.0				
8	$3.0f_b$	55.5	23.6	23.3	0.3	0.00220	−10.20
9			23.3				

Note. f_m = compressive strength of mortar and f_b = required compressive strength of concrete brick.

Table 3: Test parameters and test results.

			Test results					
	Specimen	f_m (MPa)	Compressive strength, f_{pm} (MPa)	Average of f_{pm} (MPa)	ε_0(Strain at f_{pm}	Average of ε_0	$\varepsilon_{0.5}$(strain at 0.5 f_{pm} in descend. branch)	Average of $\varepsilon_{0.5}$
1			5.310		0.0027		0.0047	
2			4.983		0.0028		0.0048	
3	Cp-2.0	$2.0f_b$	5.513	5.306	0.0027	0.0027	0.0047	0.0047
4			5.783		0.0027		0.0047	
5			4.940		0.0027		0.0047	
6			5.693		0.0027		0.0044	
7			5.439		0.0030		0.0047	
8	Cp-2.5	$2.5f_b$	5.912	5.703	0.0027	0.0029	0.0044	0.0046
9			5.418		0.0029		0.0046	
10			5.998		0.0029		0.0046	
11			5.760		0.0030		0.0047	
12			5.931		0.0030		0.0045	
13			5.868		0.0030		0.0046	
14	Cp-3.0	$3.0f_b$	5.980	5.921	0.0030	0.0030	0.0045	0.0045
15			5.825		0.0030		0.0045	
16			6.002		0.0030		0.0045	

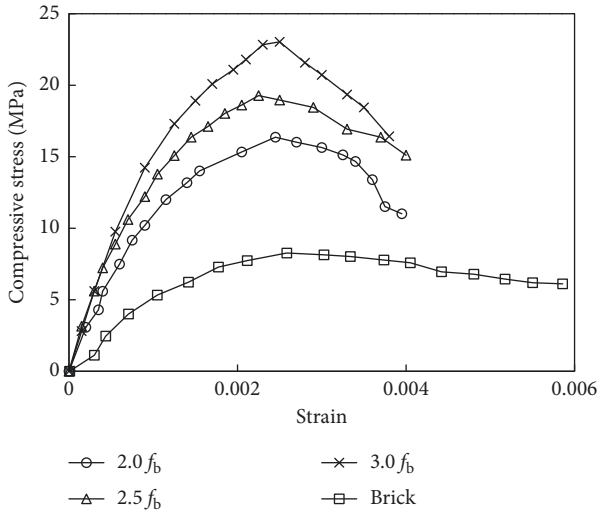

Figure 2: Compressive stress-strain curves measured in the mortars and the brick element.

sharply along the loading direction at 85% of the peak stress, which was accompanied by a rapid increase in the strain. The fracture process zone developed to the middle as reaching the peak strength. Most of the cracks were observed in the concrete bricks. At last, the cracks from one surface of the specimen developed to reach the other surface to conclude

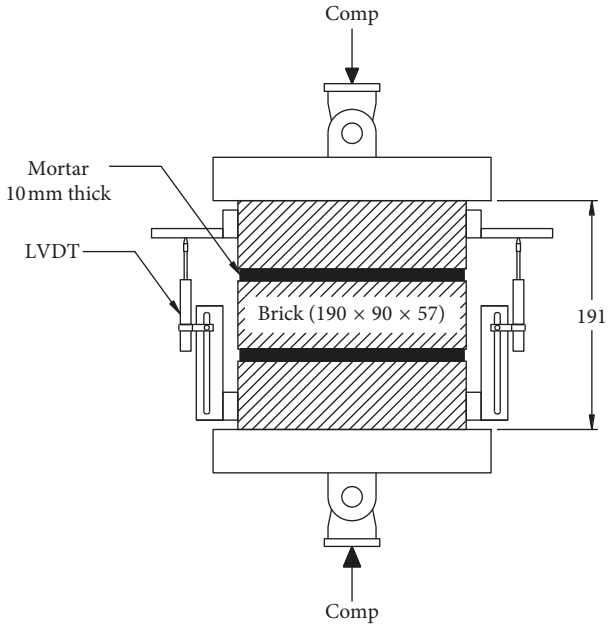

Figure 3: Concrete brick prism for compression test (unit: mm).

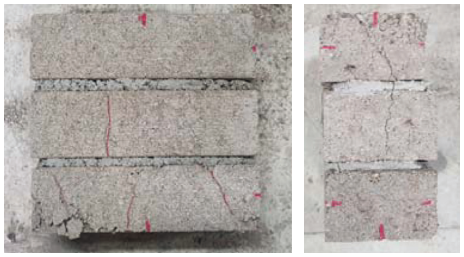

Figure 4: Typical failure mode of prism under compression.

its fracture. These tendencies were equally observed regardless of the mortar strengths.

3.2. Prism Strength. The strengths of the 16 prism specimens are listed in Table 3. Gumaste et al. [17] noted that the brick masonry strength increases with increase in brick and/or mortar strength. In this study, only one parameter, i.e., the strength of the mortar (f_m), was introduced. Because all other conditions were fixed other than that, the strength of the prism (f_{pm}) would be expressed as a function of the strength of a mortar and a brick as

$$f_{pm} = \mathbf{f}(f_m,\ f_b). \tag{1}$$

Using the test data, with a constant brick strength, a regression analysis [18] was performed as shown in Figure 5, and the relationship between the prism strength and the mortar strength was found to be

$$f_{pm} = 0.09 f_m + 3.92. \tag{2}$$

3.3. Stress-Strain Relationship. The compressive stress-strain curve of prism obtained for the concrete mixes is plotted in Figure 6. The shape of the curve was a second-degree parabola

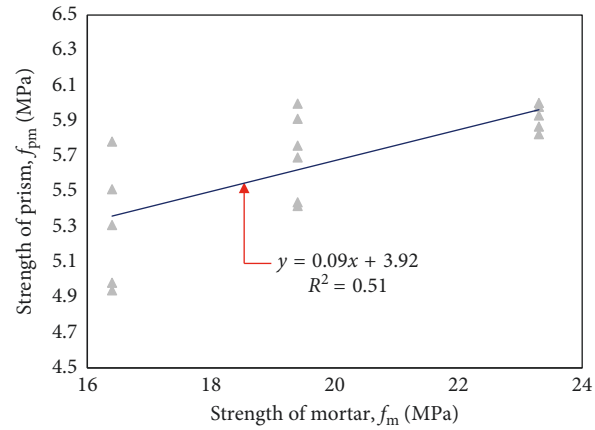

Figure 5: Regression analysis for f_{pm}.

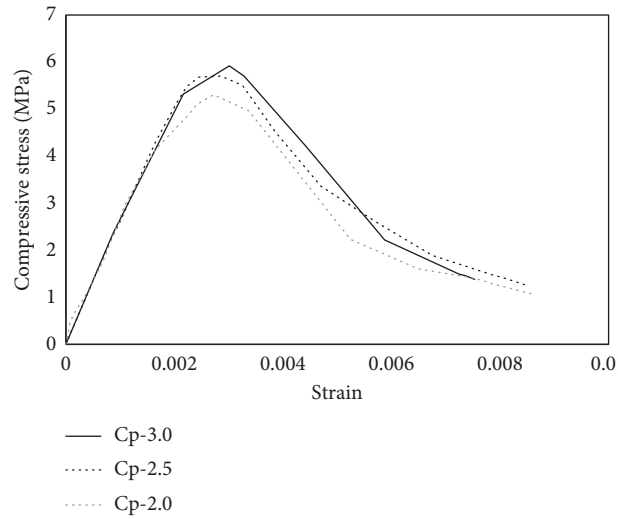

Figure 6: Compressive stress-strain curves measured in the concrete brick prism.

with its vertex at the peak stress point. The slopes of the ascending and descending branches of the curve mostly depend on f_{pm}. The curve was almost linear up to approximately one-half of the peak stress point, showing that their initial slope increased as f_{pm} increased. The strength of Cp-2.5 and Cp-3.0 were 7.3% and 11.5% higher than that of Cp-2.0, respectively. The strain at the peak stress also increased in ascending branch (the strain of Cp-2.5 and Cp-3.0 was 7.4% and 11.1% more than that of Cp-2.0, respectively) but the strain at 0.5 f_{pm} in descending branch reduced as the compressive strength increased (the strain at 0.5 f_{pm} of Cp-2.5 and Cp-3.0 was 2.1% and 4.3% less than that of Cp-2.0, respectively). It shall be noted that the strength of the prism was lower than that of the brick or mortar, against expectation. The innate nature of each materials as well as the way of assemblage of them may cause inevitable uneven contact condition and develop local cracks.

3.4. Modulus of Elasticity, E_{pm}. From above inference, it is thought that the slope of the curve in the earlier stage, i.e., the

modulus of elasticity, is directly related with the prism strength (f_{pm}). Considering a parabolic trend of the stress and strain relationship, the equation for modulus of elasticity can be expressed as

$$E_{pm} = A_1\left(f_{pm}\right)^{\alpha}\,(\text{MPa}). \tag{3}$$

Similar studies have been conducted on determining the factors A_1 and α by, for example, Yang et al. [14] and Noguchi et al. [19]. In this study, based on the test results, a regression analysis was conducted to find a best-fit value of A_1 and α in equation (3), as shown in Figure 7, finding $A_1 = 1513$ and $\alpha = 0.33$. The test results for E_{pm} and the analysis results from equation (5) are compared in Table 4. The averages of differences between them for Cp-2.0, Cp-2.5, and Cp-3.0 are 0.2%, 1.0%, and 0.9%, respectively. It can be concluded that the analysis equation for elastic modulus derived above matched with the test results with accuracy.

Equation (3) was compared with existing equations found in internationally accepted documents such as FEMA306 [20], which proposes $E_{pm} \approx 550 f_{pm}$. International Building Code [21] and the MSJC document [22] recommend E_{pm} as 700 times f_{pm}, while Eurocode6 [23] suggest conservatively higher values of E_{pm} (1,000 times f_{pm}). The Canadian masonry code S304.1 [24] recommends E_{pm} as 850 times f_{pm} with an upper limit of 20,000 MPa. The proposed E_{pm} in this study was compared with some selective existing models as shown in Figure 8. All featured models showed higher E_{pm} than the proposed model in most of the ranges of f_{pm}; in other words, the proposed model estimates the E_{pm} rather conservatively.

3.5. Strain at Peak Stress ε_0 and at 50% of Peak Stress of Descending Branch $\varepsilon_{0.5}$. MacGregor and Wight [25] established that the strain at peak stress (ε_0) of concrete increases with increase in concrete strength. The same trend is observed in brick prism made with concrete. As it was revealed from the test results shown in Table 3, for the ascending branch of the stress-strain curve, the strain at the peak stress ε_0 was proportional to f_{pm}. On the other hand, for the descending branch, $\varepsilon_{0.5}$ decreased as f_{pm} increased, i.e., they are in reverse proportion to each other. Their relationships can be expressed as

$$\varepsilon_0 = A_2 \exp\left\{B_2\left(\frac{f_{pm}}{E_{pm}}\right)\right\},$$
$$\varepsilon_{0.5} = A_3 \exp\left\{B_3\left(\frac{f_{10}}{f_{pm}}\right)\right\}, \tag{4}$$

where $f_{10} = 10$ MPa is a reference value for prism strength.

To derive equations for ε_0 and $\varepsilon_{0.5}$, nonlinear regression analysis (Figures 9 and 10) were conducted and the following best-fit equations was developed as

$$\varepsilon_0 = 0.0014 \exp\left[348\frac{f_{pm}}{E_{pm}}\right], \tag{5}$$

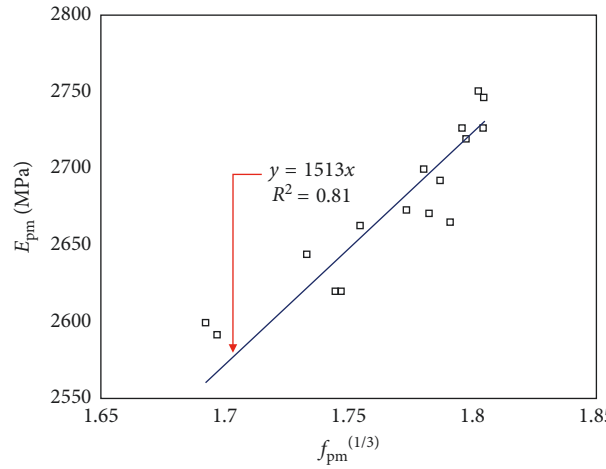

Figure 7: Regression analysis for E_{pm}.

$$\varepsilon_{0.5} = 0.004 \exp\left[0.25\left(\frac{f_{10}}{f_{pm}}\right)^{1.75}\right], \tag{6}$$

where E_{pm} is given in equation (3).

The test results for ε_0 and $\varepsilon_{0.5}$ and the analysis results from equations (5) and (6) are compared in Table 5. The averages of differences of ε_0 between them for Cp-2.0, Cp-2.5, and Cp-3.0 are 3.1%, 2.0%, and 0.7%, respectively. Those of $\varepsilon_{0.5}$ between them are 7.1%, 4.9%, 4.7%, respectively. It can be concluded that the analysis equation for strains derived above represents the test results with high fidelity.

4. Mathematical Equation for Stress-Strain Relationship

4.1. Generalized Equation. The shape of a compressive stress-strain curve of concrete is generally characterized as a parabola with its vertex at the peak stress [14]. This physically means that the tangential modulus of elasticity E_t has maximum value at the origin, gradually decreases to zero at the peak stress, and becomes negative in the descending branch of the curve (Figure 11).

In this study, the same assumption and the following nonlinear equation (7) were applied in generating a complete curve of concrete brick prism:

$$y = \frac{\beta_3 x}{x^{\beta_2} + \beta_1}, \tag{7}$$

where $y = (f_{pc}/f_{pm})$ is the normalized stress, $x = (\varepsilon_{pc}/\varepsilon_0)$ is the normalized strain, and f_{pc} is the prism stress corresponding to strain ε_{pc}.

The physical meaning of the equation gives the following boundary conditions: (1) $y = 0$, for $x = 0$; (2) $y = 1$ for $x = 1$; and (3) $(df_{pc}/d\varepsilon_{pc}) = 0$, for $x = 1$. From the first and second conditions, it can be said that β_3 is equal to $\beta_1 + 1$. From the tangential modulus at a point, $d(f_{pc})/d(\varepsilon_{pc})$, and the third boundary condition, it can be inferred that β_2 is equal to $\beta_1 + 1$. Therefore, the stress-strain curve of concrete can be expressed in the following basic form with the key parameter β_1:

Table 4: Comparison of elastic modulus from test and analysis.

	Specimen	f_m (MPa)	f_{pm} (MPa)	Elastic modulus					
				Test (MPa)	Test average (MPa)	Analysis (MPa)	Analysis average (MPa)	Difference (%)	Difference average (%)
1	Cp-2.0	$2.0f_b$	5.310	2644	2633	2640	2638	0.2	−0.2
2			4.983	2591		2584		0.3	
3			5.513	2663		2673		−0.4	
4			5.783	2670		2716		−1.7	
5			4.940	2599		2577		0.9	
6	Cp-2.5	$2.5f_b$	5.693	2673	2677	2702	2703	−1.1	−1.0
7			5.439	2620		2661		−1.6	
8			5.912	2726		2736		−0.3	
9			5.418	2620		2657		−1.4	
10			5.998	2726		2749		−0.8	
11			5.760	2700		2712		−0.5	
12	Cp-3.0	$3.0f_b$	5.931	2719	2714	2739	2737	−0.7	−0.9
13			5.868	2665		2729		−2.4	
14			5.980	2750		2746		0.1	
15			5.825	2692		2722		−1.1	
16			6.002	2746		2750		−0.1	

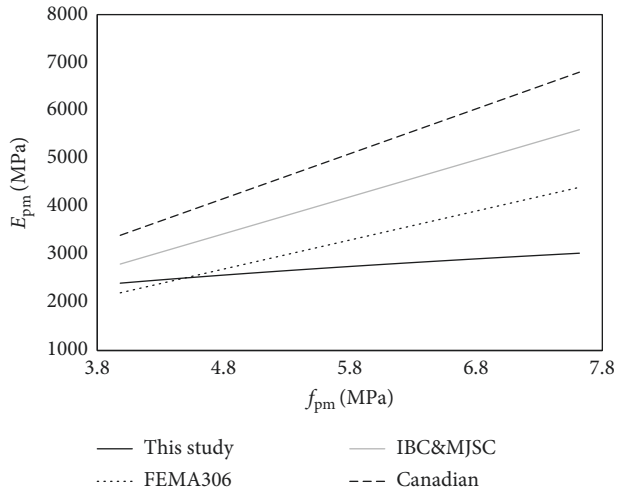

Figure 8: Comparison of proposed E_{pm} with existing models.

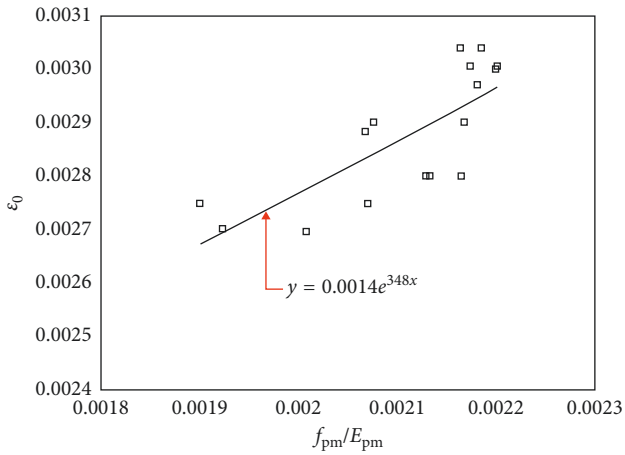

Figure 9: Regression analysis for ε_0.

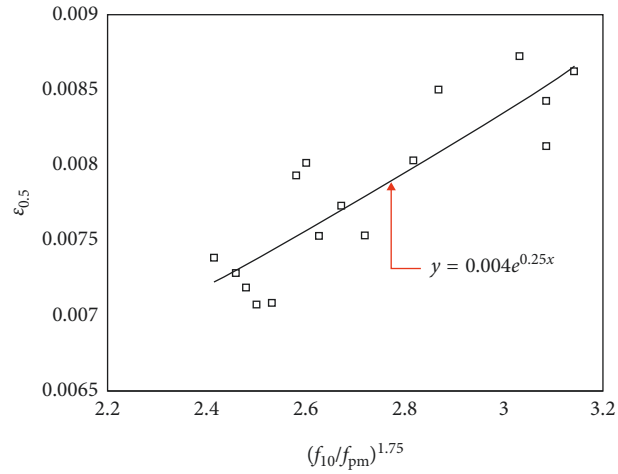

Figure 10: Regression analysis for $\varepsilon_{0.5}$.

$$y = \frac{(\beta_1 + 1)x}{x^{\beta_1+1} + \beta_1}. \tag{8}$$

Note that the slopes of the ascending and descending branches of the curve depend on the value of β_1; however, the value of β_1 differs for each branch. To determine the slope of the ascending branch, the elastic modulus of prism, E_{pm}, can be regarded as a more adequate reference parameter than the initial tangent modulus E_{ti} because of the lack of available test data for E_{ti}. Following ASTM C1314 [26], E_{pm} was decided as the slope of the line joining the 5% and the 33% of the peak strength. This statement is thought to be reasonable because the stress-strain curve of prism in compression would remain linear up to $0.33f_{pm}$ [27]. Substituting the defined E_{pm} in equation (8) gives the following equation for the key parameter β_1 of the ascending branch

$$0.4(X_a)^{\beta_1+1} + (0.4 - X_a)\beta_1 - X_a = 0, \quad \text{for } \varepsilon_{pc} \le \varepsilon_0, \tag{9}$$

where $X_a = (0.4f_{pm}/E_{pm}\varepsilon_0)$.

Table 5: Comparison of $\boldsymbol{\varepsilon}_0$ and $\boldsymbol{\varepsilon}_{0.5}$ from test and analysis.

	Specimen	f_m (MPa)	ε_0 Analysis	ε_0 Analysis average	ε_0 Difference (%)*	ε_0 Difference average (%)*	$\varepsilon_{0.5}$ Analysis	$\varepsilon_{0.5}$ Analysis average	$\varepsilon_{0.5}$ Difference (%)*	$\varepsilon_{0.5}$ Difference average (%)*
1	Cp-2.0	$2.0f_b$	0.0028	0.0028	−4.5	−3.1	0.0044	0.0044	7.1	7.1
2			0.0027		−1.3		0.0044		7.6	
3			0.0029		−4.7		0.0044		7.2	
4			0.0030		−6.2		0.0043		7.9	
5			0.0027		1.3		0.0044		5.5	
6	Cp-2.5	$2.5f_b$	0.0029	0.0029	−4.9	−2.0	0.0043	0.0044	1.4	4.9
7			0.0029		0.6		0.0044		7.0	
8			0.0030		−2.7		0.0043		1.9	
9			0.0029		0.3		0.0044		5.0	
10			0.0030		−0.3		0.0043		6.3	
11			0.0029		−5.1		0.0043		7.8	
12	Cp-3.0	$3.0f_b$	0.0030	0.0030	−0.7	0.7	0.0043	0.0043	5.0	4.7
13			0.0030		−0.3		0.0043		6.1	
14			0.0030		0.7		0.0043		4.2	
15			0.0030		2.2		0.0043		3.9	
16			0.0030		1.4		0.0043		4.3	

*The differences and the difference averages are the ones compared with the test results listed in Table 2.

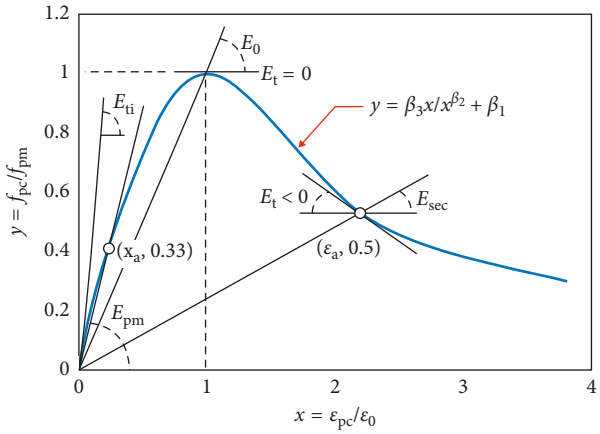

Figure 11: Generalized compressive stress-strain relationship.

In contrast to the ascending branch slope, there is no consensus on the reference point to determine the slope of the descending branch. For mathematical simplicity, Tasnimi [11] used an inflection point as a reference, but it is difficult to identify the location of the inflection point. Van Gysel and Taerwe [28] employed the secant modulus joining the origin and 50% of the peak stress to derive the descending branch slope. Furthermore, CEB-FIP [29] describes the descending branch only up to $0.5f_{pm}$ point. Following these researchers, the present study selected the secant modulus at $0.5f_{pm}$ as a reference point for evaluating the descending branch slope and formulated an equation for the key parameter β_1 defining the descending branch as follows:

$$(X_d)^{\beta_1+1} + (1 - 2X_d)\beta_1 - 2X_d = 0, \quad \text{for } \varepsilon_{pc} > \varepsilon_0, \tag{10}$$

where $X_d = (\varepsilon_{0.5}/\varepsilon_0)$ and $\varepsilon_{0.5}$ is the strain corresponding to $0.5f_{pm}$ after the peak stress.

The value of β_1 in nonlinear equations (9) and (10) can be calculated via numerical analysis, such as the Newton–Raphson method, using the given values of f_{pm}.

4.2. Key Parameter β_1. The equations for E_c, ε_0, and $\varepsilon_{0.5}$ derived in the preceding subsections were substituted in equations (9) and (10). These two nonlinear equations, which incorporate f_{pm}, were then solved for β_1 using the Newton–Raphson method. Based on the analytically obtained results, a statistical optimization was carried out as shown in Figure 12 to derive the following best-fit equations for β_1: equation (5) for the ascending branch and equation (6) for the descending branch.

$$\beta_1 = 0.62 \exp\left\{0.91\left(\frac{f_{pm}}{f_{10}}\right)^{0.67}\right\}, \quad \text{for } \varepsilon_{pc} \le \varepsilon_0, \tag{11}$$

$$\beta_1 = 0.31 \exp\left\{1.53\left(\frac{f_{pm}}{f_{10}}\right)^{0.67}\right\}, \quad \text{for } \varepsilon_{pc} > \varepsilon_0. \tag{12}$$

In summary, a stress-strain relationship model for the prism in compression is proposed as follows:

$$f_{pc} = \frac{(\beta_1 + 1)\left(\varepsilon_{pc}/\varepsilon_0\right)}{\left(\varepsilon_{pc}/\varepsilon_0\right)^{\beta_1+1} + \beta_1} f_{pm}, \tag{13}$$

where ε_{pc} is a strain, ε_0 is given by equation (5), and β_1 is given by equations (11) or (12).

4.3. Comparisons with Existing Models. In this section, the test and analysis results provided above are compared with another notable model. Knutson [8] assessed the masonry stress-strain diagram for different combinations of mortar and brick and concluded that the stress-strain relationship could be approximated as

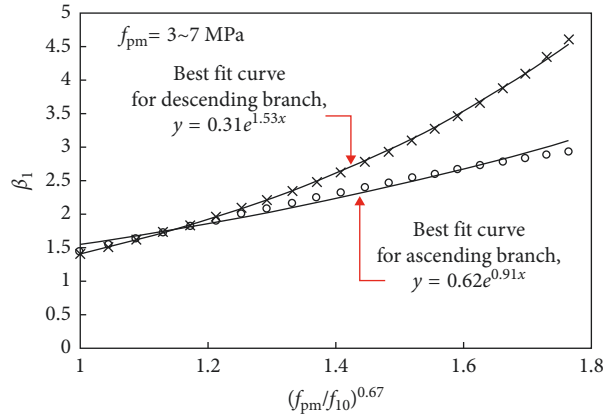

Figure 12: Best-fit equation for key parameter β_1 obtained from numerical analysis.

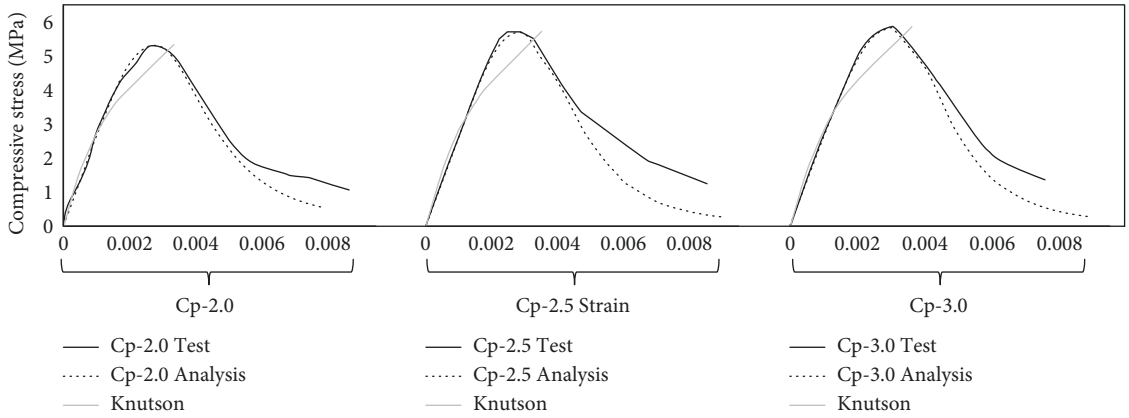

Figure 13: Comparisons of predicted stress-strain curves with test results.

$$\varepsilon = -\frac{f_{cmas}}{E_0}\ln\left(1-\frac{\sigma}{f_{cmas}}\right), \quad \text{if } \frac{\sigma}{f_{cmas}} \le 0.75,$$
$$\varepsilon = -4\frac{f_{cmas}}{E_0}\left(0.403-\frac{\sigma}{f_{cmas}}\right), \quad \text{if } \frac{\sigma}{f_{cmas}} > 0.75, \tag{14}$$

where σ is the normal stress, ε is the normal strain, f_{cmas} is the masonry compressive strength, and E_0 is the elastic modulus.

The stress-stain relationship of the test specimens and the analytical results from the proposed model and Knutson's model are compared in Figure 13. The normalized root-mean-square errors obtained from each stress-strain curve are listed in Table 6.

The stress-strain graphs generated by the analysis model match with the test results quite well from the beginning, through ascending branch, to the 50% of peak stress in the descending branch. In the final stage after the $\varepsilon_{0.5}$ in the descending branch, the analysis results showed rather decreased ductility than the test results. It is thought that the confined condition of the specimens in test affected the ductility after the crush had happened. Further experimental study with mode specimens under same or different test set-ups is required to find out the cause of difference.

Table 6: Comparisons of normalized root-mean-square error obtained from each stress-strain curve.

Specimen	f_m (MPa)	Researcher	
		This study	Knutson
Cp-2.0	$2.0f_b$	0.249	0.357
Cp-2.5	$2.5f_b$	0.257	0.351
Cp-3.0	$3.0f_b$	0.239	0.358

Note. Normalized root-mean-square error (NRMSE) = $(1/(f_{pm})_m)\sum[\{(f_{pm})_{Exp}-(f_{pm})_{Pre}\}^2/n]^{1/2}$, where $(f_{pm})_m$ is the mean stress in the measured stress-strain curve, $(f_{pm})_{Exp}$ and $(f_{pm})_{Pre}$ are experimental and predicted stress, respectively, and n is number of points in experimental stress-strain curve.

The Knutson model would deal with the stress-strain relationship of the brick prism from loading commencement, only up to the peak stress. The curve matched with the test results well until 60% of the peak stress. After that, the decreased stiffness moved the peak point far away from that of the tests. For example, the strain at the peak point from the Knutson model was 23% more than that from the test of specimen Cp-2.5. The model did not provide the descending branch of a stress-strain curve.

In summary, the above comparison reveals some limitations of Knutson's model: (1) only ascending branch can be modeled in Knutson's model, as is often the case with; (2)

compared with the earlier stage of the stress-strain relationship, the final stage of it is not well explained. On the other hand, the predictions from the model proposed in this study are in better agreement regardless of compressive strength. The calculated normalized root-mean-square error (NRMSE) by the proposed model ranged between 0.239 and 0.257, while in Knutson model, it was between 0.357 and 0.358 (Table 6).

5. Conclusions

In this study, concrete brick prisms with three different mortar strengths and with the same brick strength were tested under compressive load. An analytical model was proposed to provide a stress-strain relationship of them. Based on the research summarized in this paper, the following conclusions were drawn:

(1) The compressive strength of the prism differed according to the mortar strength when the brick unit strength was constant. However, the increase rate of the prism strength was not exactly proportional to the increase rate of the mortar.

(2) The strength of a brick prism was not a summation of both brick strength and mortar strength. Rather, it was lower than the individual strength of a brick unit or a mortar. The contact condition of both nonhomogeneous materials is thought to cause local cracks under compressive condition.

(3) The proposed stress-strain model for brick prism in compression predicted the relationship accurately, regardless of mortar strength, although some discrepancies were observed after $\varepsilon_{0.5}$ in the descending branch.

(4) The key parameter β_1, which is an exponential function of $(f_{pm})^{0.67}$, defines the stress-strain curve. Two equations for β_1 were provided for ascending and descending branches, separately.

(5) The proposed stress-strain relationship model contributes towards the mathematical simplicity of analytical modeling.

(6) The authors considered that the comparison between Ewing and Kowalski [10], Kaushik et al.'s [27] modeling based on the "modified" Kent–Park model proposed by Priestley and Elder [30], and their own model should be given on a future assignment.

Data Availability

The data used to support the findings of this study are included within the article.

Conflicts of Interest

The authors declare that they have no conflicts of interest.

Acknowledgments

This research was supported by the Basic Science Research Program through the National Research Foundation of Korea (NRF) funded by the Ministry of Science, ICT & Future Planning (no. 2015R1A5A1037548) and by Kyonggi University's Graduate Research Assistantship 2018.

References

[1] R. H. Atkinson, J. L. Noland, D. P. Abrams, and S. McNary, "A deformation failure theory for stack-bond brick prisms in compression," in *Proceedings of 3rd NAMC*, Arlington, TX, USA, 1985.

[2] P. Kumar, "A compact analytical material model for unconfined concrete under uni-axial compression," *Materials and Structures*, vol. 37, no. 9, pp. 585–590, 2004.

[3] M. A. Mansur, T. H. Wee, and M. S. Chin, "Derivation of the complete stress-strain curves for concrete in compression," *Magazine of Concrete Research*, vol. 47, no. 173, pp. 285–290, 1995.

[4] S. M. Palmquist and C. Jansen, "Postpeak strain-stress relationship for concrete in compression," *ACI Materials Journal*, vol. 98, no. 3, pp. 213–219, 2001.

[5] S.-T. Yi, J.-K. Kim, and T.-K. Oh, "Effect of strength and age on the stress-strain curves of concrete specimens," *Cement and Concrete Research*, vol. 33, no. 8, pp. 1235–1244, 2003.

[6] S. Popovics, "A numerical approach to the complete stress-strain curve of concrete," *Cement and Concrete Research*, vol. 3, no. 5, pp. 583–599, 1973.

[7] M. Sargin, S. K. Ghosh, and V. K. Handa, "Effects of lateral reinforcement upon the strength and deformation properties of concrete," *Magazine of Concrete Research*, vol. 23, no. 75-76, pp. 99–110, 1971.

[8] H. H. Knutson, "The stress-strain relationship for masonry," *Masonry International*, vol. 7, no. 1, pp. 31–33, 2003.

[9] G. Mohamad, P. B. Lourenco, and H. R. Roman, "Mechanical behavior assessment of concrete block masonry prisms under compression," in *Proceedings of International Conference for Structures*, pp. 261–268, Coimbra, Portugal, 2005.

[10] B. D. Ewing and M. J. Kowalsky, "Compressive behavior of unconfined and confined clay brick masonry," *Journal of Structural Engineering*, vol. 130, no. 4, pp. 650–661, 2004.

[11] A. A. Tasnimi, "Mathematical model for complete stress-strain curve prediction of normal, light-weight and high-strength concretes," *Magazine of Concrete Research*, vol. 56, no. 1, pp. 23–34, 2004.

[12] A. J. Aref and K. M. Dolatshahi, "A three-dimensional cyclic meso-scale numerical procedure for simulation of unreinforced masonry structures," *Computers and Structures*, vol. 120, pp. 9–23, 2013.

[13] S. Burnett, M. Gilbert, T. Molyneaux, G. Beattie, and B. Hobbs, "The performance of unreinforced masonry walls subjected to low-velocity impacts: finite element analysis," *International Journal of Impact Engineering*, vol. 34, no. 8, pp. 1433–1450, 2007.

[14] K. H. Yang, J. H. Mun, M. S. Cho, and T. H. Kang, "Stress-strain model for various unconfined concrete in compression," *ACI Structural Journal*, vol. 111, no. 4, pp. 819–826, 2014.

[15] Korean Standard Association, *KS F404 Concrete Bricks*, Korean Standard Association, Seoul, South Korea, 2013.

[16] Korean Standard Association, *KS L5220 Dry Ready Mixed Cement Mortar*, Korean Standard Association, Seoul, South Korea, 2013.

[17] K. S. Gumaste, K. S. N. Rao, B. V. V. Reddy, and K. S. Jagadish, "Strength and Elasticity of brick masonry prisms and wallettes

under compression," *Materials and Structures*, vol. 40, pp. 241–253, 2004.

[18] A. H.-S. Ang and W. H. Tang, *Probability Concepts in Engineering Planning and Design, Volume I–Basic Principles*, John Wiley and Sons, Inc., Hoboken, NJ, USA, 1975.

[19] T. Noguchi, F. Tomosawa, K. M. Nemati, B. M. Chiaia, and A. P. Fantilli, "A practical equation for elastic modulus of concrete," *ACI Structural Journal*, vol. 106, no. 5, pp. 690–696, 2009.

[20] Federal Emergency Management Agency (FEMA), *Evaluation of Earthquake Damaged Concrete and Masonry Wall Buildings, Basic Procedures Manual*, ATC-43, FEMA 306, Applied Technology Council, Redwood City, CA 94065, USA, 1999.

[21] International Code Council, *International Building Code*, International Code Council, Virginia Beach, VA, USA, 2003.

[22] Masonry Standards Joint Committee (MSJC), *Building Code Requirements for Masonry Structures*, ACI 530-02/ASCE 5-02/TMS 402-02, American Concrete Institute, Structural Engineering Institute of the American Society of Civil Engineers, The Masonry Society, Detroit, MI, USA, 2002.

[23] European Committee of Standardization (CEN), *Design of Masonry Structures. Part 1-1: General Rules for Buildings—Reinforced and Unreinforced Masonry*, ENV 1996-1-1, Eurocode 6, Brussels, Belgium, 1996.

[24] Canadian Standards Association (CSA), *Design of Masonry Structures, S304.1*, Canadian Standards Association (CSA), Ontario, Canada, 2004.

[25] J. G. MacGregor and J. K. Wight, *Reinforced Concrete: Mechanics and Design*, Prentice-Hall, New York, NY, USA, 2006.

[26] ASTM C1314, *Standard Test Method for Compressive Strength of Masonry Prisms*, ASTM International, West Conshohocken, PA, USA, 2018.

[27] H. B. Kaushik, D. C. Rai, and S. K. Jain, "Stress-strain characteristics of clay brick masonry under uniaxial compression," *Journal of materials in civil engineering*, vol. 19, no. 9, pp. 728–739, 2007.

[28] A. Van Gysel and L. Taerwe, "Analytical formulation of the complete stress-strain curve for high strength concrete," *Materials and Structures*, vol. 29, no. 9, pp. 529–533, 1996.

[29] Committee Euro-International du Beton (CEB-FIP), *Structural Concrete: Textbook on Behavior, Design and Performance*, International Federation for Structural Concrete (FIB), Lausanne, Switzerland, 1999.

[30] M. J. N. Priestley and D. M. Elder, "Stress-strain curves for unconfined and confined concrete masonry," *Journal of the American Concrete Institute*, vol. 80, no. 3, pp. 192–201, 1983.